# Molecular-beam infrared–infrared double-resonance spectroscopy study of the vibrational dynamics of the acetylenic C–H stretch of propargyl amine

Anne M. Andrews, Gerald T. Fraser, and Brooks H. Pate

Citation: The Journal of Chemical Physics **109**, 4290 (1998); doi: 10.1063/1.477033
View online: http://dx.doi.org/10.1063/1.477033
View Table of Contents: http://scitation.aip.org/content/aip/journal/jcp/109/11?ver=pdfcov
Published by the AIP Publishing

# Molecular-beam infrared–infrared double-resonance spectroscopy study of the vibrational dynamics of the acetylenic C–H stretch of propargyl amine

Anne M. Andrews,[a] Gerald T. Fraser, and Brooks H. Pate[b]
*Molecular Physics Division, National Institute for Standards and Technology, Gaithersburg, Maryland 20899*

(Received 4 September 1997; accepted 10 June 1998)

The acetylenic C–H stretch spectrum of propargyl amine near 3330 $cm^{-1}$ has been measured at 0.0002 $cm^{-1}$ (6 MHz) resolution with a tunable color-center laser in an electric-resonance optothermal spectrometer. The spectrum has been fully assigned through IR–IR double resonance measurements employing a tunable, microwave sideband-$CO_2$ laser. The 10 $\mu$m spectrum of propargyl amine displays splittings in the two nuclear spin symmetry states arising from amino-proton interchange, allowing double-resonance assignment of the $-NH_2$ group resultant proton nuclear spin quantum number in the highly fragmented 3 $\mu$m spectrum. The experimental state density is consistent with a $(2J+1)$ increase that is expected if all near-resonant states are coupled. From this $J$-dependent growth in the state density we determine the density of states at $J=0$ to be 22 states/$cm^{-1}$. This value is in reasonable agreement with the direct state count result of 16 states/$cm^{-1}$. The unperturbed transition frequencies for the two different nuclear spin species at a given rotational level do not coincide, differing on average by about 50 MHz. The nonresonant coupling effects which produce effective splittings in the 10 $\mu$m spectrum appear to survive into the high state density regime. The measured IVR lifetimes are on the order of 500 ps for the low $K_a$ values studied here $(K_a<4)$ and show a $K_a$-dependence with the IVR rate increasing as $K_a$ increases. The statistical properties of the spectrum have been compared to predictions from random matrix theory. The level spacings are not well represented by Wigner statistics as would be expected for underlying chaotic classical dynamics. However, the intensity fluctuations are consistent with a $\chi^2$-distribution, expected for classically chaotic systems, as measured by Heller's F-statistic.
 [S0021-9606(98)01035-6]

## I. INTRODUCTION

The vibrational dynamics of isolated molecules is a subject of long standing interest in chemical physics. Much of the interest comes from the study of unimolecular reactions where statistical models, such as the Rice, Ramsperger, Kassel, and Marcus (RRKM) theory, have been extremely successful in calculating reaction rates.[1] These statistical theories assume that vibrational energy is redistributed within the molecule on a time scale that is rapid compared to reaction. The vibrational dynamics of polyatomic molecules are also important for bimolecular chemistry. As with unimolecular reactions, mode-specific effects may be observed when the time scale for intramolecular vibrational energy redistribution (IVR) is slow compared to reaction times. For some bimolecular reactions the vibrational excitation can be localized in the reacting bond using optical excitation. In this way, a few laser-induced, bond-specific bimolecular reactions of small molecules, where IVR does not occur, have been achieved.[2–4] The determination of energy localization lifetimes in larger polyatomic molecules, and the ability to calculate these lifetimes,[5] is of central importance to both unimolecular and bimolecular reaction dynamics.

Molecular-beam, frequency-resolved measurements of the infrared spectra of large polyatomic molecules can provide information on the IVR process.[6–9] Over the past few years a number of ''IVR lifetimes,'' which determine the time scale of energy localization in a specific bond mode, have appeared.[10] These IVR lifetimes can be determined once the molecule is large enough to provide a background density of states that can act as a bath for the energy redistribution. This vibrational bath is composed of the numerous overtone and combination bands of the lower-lying normal mode vibrations in the energy region of the bond-mode vibration of interest. Experimental evidence indicates that IVR is observable through extensive near-resonant perturbations in the frequency-resolved spectrum once the vibrational state density is on the order of 10 states/$cm^{-1}$ to 100 states/$cm^{-1}$.[6–11]

The IVR process, as studied here, is concerned with the dynamics of bound states and, therefore, there is no lifetime broadening of the individual eigenstates measured in the frequency-resolved spectrum (except the fluorescence lifetime broadening due to the coupling to the radiation continuum).[12] A fully-resolved spectrum in the IVR regime shows that instead of a single rovibrational transition, a set of transitions, an ''IVR multiplet'' is observed. This set of

[a]Current address: Institute for Defense Analysis, 1801 N. Beauregard, Alexandria, VA 22311-1772.
[b]Current address: Department of Chemistry, University of Virginia, Charlottesville, VA 22901.

 

eigenstates results from the near-resonant mixing of the vibrational states. The time-dependent behavior is associated with the production of a coherent state by a wide bandwidth (short pulse) laser. In cases where a single, zeroth-order rovibrational state carries the oscillator strength (the bright state), a short pulse excitation can create an initial superposition state with this zeroth-order identity. The probability of finding the molecule in this zeroth-order state, typically a normal or local mode vibrational state, will have a time dependence. The decay of this probability is the IVR process.

When the vibrational bath state density is higher than the reciprocal of the natural linewidth a true continuum exists and there is energy relaxation.[12] In this case a Lorentzian line shape will be observed and the connection between the linewidth and the IVR lifetime is well-known. However, at lower bath state densities the individual molecular eigenstates can be measured. This regime is frequently called intermediate-case IVR and is the regime considered here in the acetylenic C–H spectrum of propynylamine (propargyl amine, $H–C{\equiv}C–CH_2NH_2$). For intermediate-case spectra, a lifetime can be determined by calculating the time-dependent survival probability.[10] This lifetime is still related to the frequency width over which the individual eigenstates are observed.

The interpretation of a frequency-resolved spectrum in terms of the vibrational dynamics requires a complete assignment of the spectrum. Assignment of all good quantum numbers removes ambiguities that occur in interpreting low resolution spectra where inhomogeneous effects, such as hot band absorptions, can dominate the appearance of the spectrum. Once a full assignment is available, state-dependent properties of the intramolecular dynamics, not just rotationally averaged quantities, can be determined. In the case of propargyl amine, full assignment includes the nuclear spin label associated with the feasible operation of amino-proton interchange. In the ground vibrational state the tunneling process of these equivalent protons does not result in a splitting of the rotational transitions.[13] As a result, neither ground state combination differences nor infrared-microwave double-resonance techniques can be used to make the full assignment of the 3 $\mu$m spectrum. However, the 10 $\mu$m spectrum of propargyl amine shows tunneling splittings.[14] The presence of these splittings means that infrared–infrared double-resonance measurements can supply the full assignments.

The present spectrum of the acetylenic C–H stretch of propargyl amine provides an interesting example of the vibrational dynamics of a molecule in the intermediate case of intramolecular vibrational energy redistribution. The presence of two nuclear-spin modifications of propargyl amine means that there are two independent, superimposed spectra. The density of states for the two modifications are expected to be approximately equal. The total intensity for the transitions arising from the triplet and singlet species will be in the 3:1 ratio dictated by the spin statistics. Therefore, an estimate of the completeness of the assignment is available since, on average, there will be an equal number of transitions making up the IVR multiplet and the intensity sum should show a 3:1 ratio.

In addition, the fully assigned spectrum can be used to assess the importance of the large amplitude motions in the vibrational dynamics of the acetylenic C–H stretch. Evidence of strong couplings to highly-excited states of the large amplitude motion can appear in the center-of-gravity splittings of the singlet and triplet IVR multiplets. Also, due to the presence of tunneling splittings in many of the background bath states, the exact identity of the vibrational bath states very nearly resonant with the bright state, that is within the IVR linewidth of about 1 GHz, is expected to be different for the two spin modifications. However, the bath structure of the longer range coupling, involving states off-resonance by a few wave numbers, is expected to be very similar for the two spin modifications. Comparison of the IVR lifetimes for the two spin modifications provides an indirect measure of the relative importance of local and nonlocal vibrational interactions in determining the IVR lifetime.

## II. EXPERIMENT

The 3.0 $\mu$m acetylenic C–H stretch spectrum of 2-propynylamine (propargyl amine, $HC{\equiv}CCH_2NH_2$) was measured using an electric-resonance optothermal spectrometer (EROS).[15] The molecular beam was formed by expanding a 5% mixture of propargyl amine in He through a 60 $\mu$m nozzle at a 100 kPa (1 atm) backing pressure. The output of a tunable, single-mode color-center laser (7 mW) is multipassed (15 crosses) through the molecular beam using 2 cm plane-parallel mirrors. The multipass cell is located in the source chamber between the nozzle and skimmer. The linewidths of the 3.0 $\mu$m transitions are about 6 MHz. The frequencies of the transitions are determined using a wavemeter for absolute frequency calibration and a 150 MHz confocal étalon to provide relative frequencies. The wavemeter limits the transition frequency accuracy to $\pm 0.01$ cm$^{-1}$, however, spacings between transitions within a single scan [which covers the region of a single $P(J)$ or $R(J)$ transition] are precise to about 3 MHz. Previous experience with the spectrometer indicates that the intensity of the transitions are precise to about $\pm 10\%$ of the peak intensity.

After the skimmer, the molecular beam passes through a 56 cm long state-focusing assembly of quadrupolar symmetry. Molecules in the ground vibrational state are deflected according to their Stark effect behavior, however, molecules which have been excited to eigenstates of the acetylenic C–H stretch travel through the state-focusing assembly without deflection.[16] The observed signals are, therefore, only a function of the transition strength and the focusing properties of the ground rotational state. In the present study, this means that the focusing characteristics of the two nuclear spin modifications of propargyl amine for a given rotational level are identical since the rotational spectrum of the two forms are equivalent at the experimental microwave resolution (100 kHz).[13] The nonfocusing behavior of the vibrationally excited eigenstates insures that the relative intensities of a set of eigenstates arising from multiple perturbations to a single rovibrational excited state reflect the transition dipole moment distribution. This relative intensity information must be valid for a dynamical interpretation of the spec-

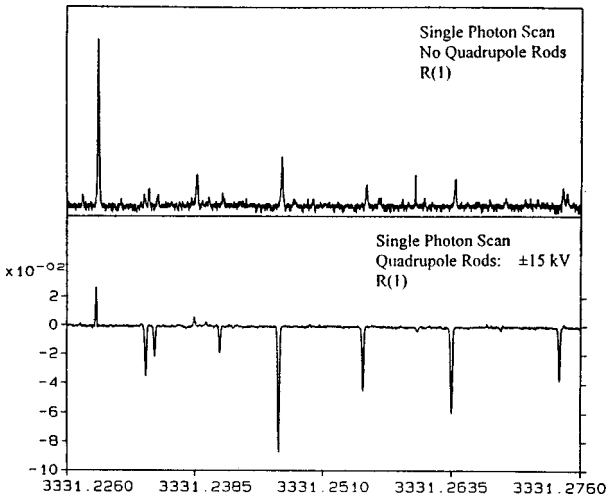


FIG. 1. A part of the $R(1)$ region of the acetylenic C–H stretch spectrum near 3331.25 $cm^{-1}$ is shown. In the top panel the spectrum is measured without any voltage on the quadrupole rods. In the bottom panel, the same region is scanned with ±15 kV applied. Transitions assigned to $2_{11}-1_{10}$ (see Fig. 2) are enhanced by a factor of 11 and change direction. These transitions come from a focusing ground state ($1_{10}$) and terminate on nonfocusing eigenstates. Because of the nonfocusing behavior of the eigenstates in the IVR regime, the relative intensities of transitions arising from the same ground rotational state are the same in the two spectra.

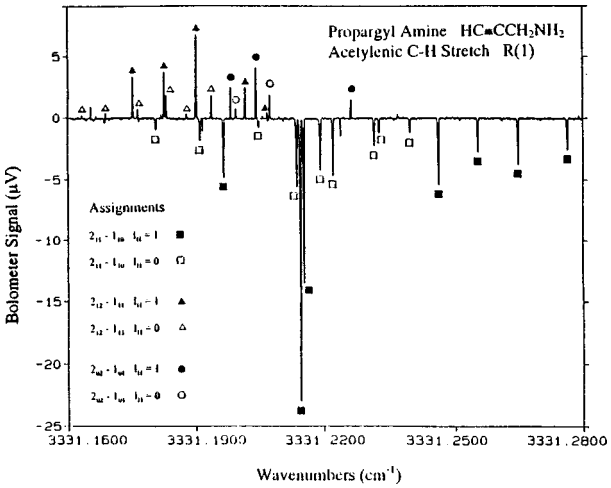


FIG. 2. The $R(1)$ region of the acetylenic C–H stretch of propargyl amine around 3331.22 $cm^{-1}$ is shown. The linewidth of the transitions is about 0.0002 $cm^{-1}$ (6 MHz). The spectrum has been assigned through IR–IR double resonance using the 10 $\mu$m spectrum of propargyl amine. Since the 10 $\mu$m spectra show frequency splittings for the two different torsion-inversion states ($I_H=1$ and $I_H=0$), the 3.0 $\mu$m spectrum can be fully assigned. This complete assignment is necessary for the dynamical IVR interpretation of the eigenstate spectrum. The frequency degeneracy between the two spin species is lifted in the 3.0 $\mu$m region because of different local bath state structure. Each eigenstate can be uniquely assigned to either the triplet ($I_H=1$) or singlet ($I_H=0$) spin species of the torsion-inversion states.

trum. A portion of the spectrum in the region of $R(1)$ is shown in Fig. 1 both with and without the quadrupole fields.

In the present configuration, no beam stop (or stopwire) is used to block the nonfocusing central portion of the molecular beam. In this case, the nonfocusing behavior gives rise to bidirectional signals in the 3.0 $\mu$m region; Negative signals come from excitation out of ground rotational states that are focused by the quadrupole fields (states with positive Stark coefficients).[17] In this case, the ground state is collected with an enhanced solid angle, providing a larger beam flux to the bolometer detector. Upon vibrational excitation, the collection solid angle is reduced to the solid angle of the bolometer detector itself. There is an energy loss at the detector due to this reduction in collected beam flux. Similarly, positive signals occur for vibrational excitation out of ground rotational states which defocus (states with negative Stark coefficients). In this case, there is initially no beam flux reaching the detector. Vibrational excitation permits collection of the molecules in the detector solid angle. An increase in energy at the bolometer is measured as these molecules deliver their kinetic energy, vibrational energy, and their energy of adsorption to the bolometer. The full region of $R(1)$ is shown in Fig. 2, with assignments, to illustrate these bidirectional signals.

All assignments are made through infrared–infrared double resonance measurements with the 3.0 $\mu$m color center laser and a microwave-sideband $CO_2$ laser. The sideband $CO_2$ laser provides frequency coverage 6 GHz to 18 GHz above and below each $CO_2$ laser line.[18] The output of this laser (~1 mW) is also sent through the plane-parallel multipass cell in the source chamber. The tunable 10 $\mu$m radiation and 3.0 $\mu$m radiation enter the spectrometer the opposite sides. The two laser beams counter propagate along the same path providing good spatial overlap of the two excitation sources.

For double-resonance measurements, the $CO_2$ sideband laser output is 100% amplitude modulated and set to an assigned transition of propargyl amine.[14] The signal of this transition is monitored through phase-sensitive detection as the color-center laser is scanned without modulation. Changes in the 10 $\mu$m signal strength occur when the 10 $\mu$m and 3.0 $\mu$m transitions share a common ground rotational state. Sequential excitations to the 4000 $cm^{-1}$ region are not observed and are likely shifted 1 $cm^{-1}$ to 10 $cm^{-1}$ from the acetylenic C–H stretch fundamental frequency by anharmonicity. An example of a double-resonance scan is presented in Fig. 3. Since tunneling splittings are resolved in the 10 $\mu$m spectrum, full quantum labels ($J$, $K_a$, $K_c$, and $I_H$) can be assigned to the eigenstates at 3.0 $\mu$m. The noise limit in the double-resonance experiments is determined by the stability of the sideband laser. Therefore, the noise is proportional to the 10 $\mu$m signal strength. This results in nearly equal sensitivity for assignment of the singlet ($I_H=0$) and triplet ($I_H=1$) nuclear spin species arising from amino-proton interchange, despite the 3:1 intensity ratio of triplet-to-singlet transitions in the single photon spectrum.

## III. THE 10 $\mu$m SPECTRUM OF PROPARGYL AMINE

The 10 $\mu$m spectrum of propargyl amine has been presented in a previous paper which also considered the spectrum of cyclopropyl amine.[14] This paper discussed the nature of the two coupled large amplitude motions in primary amines; internal rotation about the C–N bond and inversion at the amino nitrogen. An interesting feature of the dynamics of primary amines is that amino-proton interconversion must

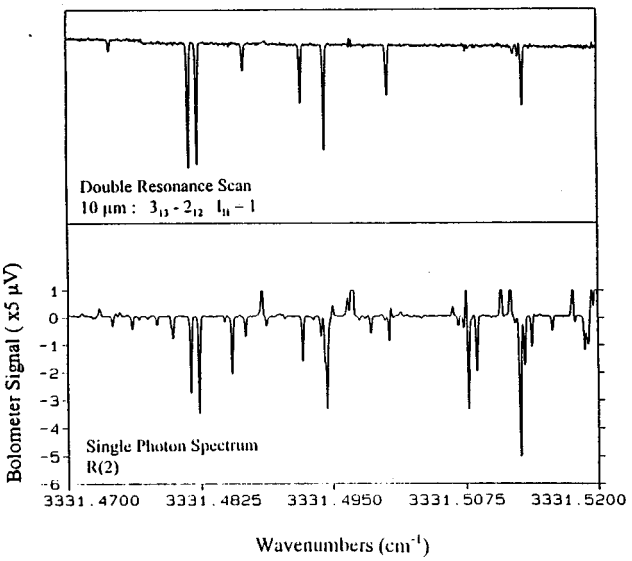


FIG. 3. An example of a double resonance scan in the $R(2)$ region of the spectrum near 3331.49 $cm^{-1}$ is presented. The bottom panel shows the single photon spectrum in the $R(2)$ region. The positive-going peaks have been clipped off. The top panel shows the same frequency region scanned in double resonance. The amplitude modulated sideband-$CO_2$ laser is set to the frequency of the $3_{13}-2_{12}$, $I_H=1$ transition of the 931 $cm^{-1}$ band of propargyl amine. The color center laser is scanned without modulation. Decreases in the 10 $\mu$m signal are observed when 3.0 $\mu$m transitions sharing the same $2_{12}$, $I_H=1$ ground state are encountered. A simplified and fully assigned spectrum of the 3.0 $\mu$m, $3_{13}-2_{12}$, $I_H=1$ is obtained. This transition is composed of several molecular eigenstates which result from extensive vibrational coupling to near-resonant bath states.

occur through a concerted inversion-internal rotation process.[19] Unlike the case of threefold rotors, simple internal rotation is insufficient to cause proton interconversion. The two limiting-case pathways for reaching isoenergetic structures are depicted in Fig. 4.

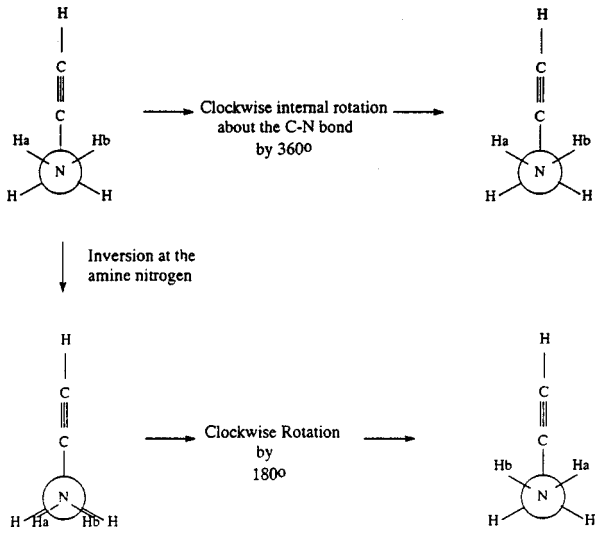


FIG. 4. Two pathways for intramolecular motion that recover isoenergetic structures of the more stable *trans* conformer of propargyl amine are depicted. Internal rotation about the C–N bond is shown across the top of the figure. This internal motion does not interconvert the amino-protons. The two different nuclear spin species, which result from amino-proton interconversion, arise from the concerted inversion-internal rotation motion sketched in the other pathway.

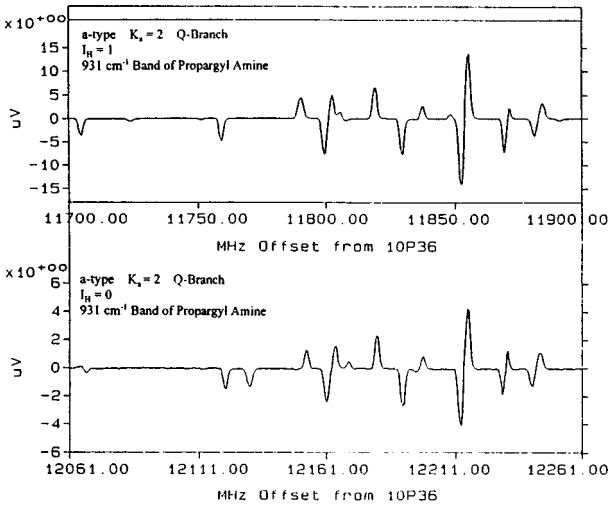


FIG. 5. The *a*-type $K_a=2$ *Q*-branches for the two different spin species in the 931 $cm^{-1}$ band of propargyl amine are shown. The linewidth of the transitions is about 0.0001 $cm^{-1}$ (3 MHz). The spectrum for the triplet ($I_H=1$) species is three times the intensity of the singlet ($I_H=0$) spectrum as expected by the spin weights. The two *Q*-branches are shifted by about 360 MHz relative to each other. This shift is $K_a$-dependent. However, the shift is relatively *J*-independent as seen by the similarity in the two spectra. In the 10 $\mu$m region the frequency degeneracy of the two spin species is lifted by nonresonant couplings to the bath, however, the spectrum remains unfragmented since the low bath state density is insufficient for extensive near-resonant coupling.

The high-barrier associated with the $-NH_2$ proton interchange prevents measurable tunneling splittings in the pure rotational spectrum of propargyl amine. However, significant tunneling splittings are observed in the vibrations near 1000 $cm^{-1}$.[14] The tunneling rate is presumably enhanced in this spectral region because of the presence of the $-NH_2$ wag fundamental.[20] This vibration provides excitation within the large amplitude surface parameterized by the internal rotation and inversion coordinates making tunneling more facile. For the purposes of the measurements reported here it is sufficient to note that transitions to the singlet ($I_H=0$) and triplet ($I_H=1$) nuclear spin states are well-separated (on the order of 500 MHz splitting). A portion of the 931 $cm^{-1}$ band of propargyl amine is shown in Fig. 5 to illustrate the splitting and 3:1 intensity ratio in the spectrum of the two nuclear-spin species.

## IV. RESULTS

Transitions of the acetylenic C–H stretch of propargyl amine were assigned for upper-state $J$ values of $0 \leqslant J \leqslant 4$ using the $P(1)$, $P(2)$, $R(1)$, $R(2)$, and $R(3)$ regions of the *a*-type spectrum. The $P(2)$, $R(2)$, and $R(3)$ spectral regions are shown in Fig. 6 [the $R(1)$ region appears in Fig. 2]. Since hyperfine structure due to the *N* atom is not resolved, the total angular momentum is denoted as *J*. Table I provides the number of eigenstates making up each IVR multiplet, the center-of-gravity frequency position, and the intensity ratios of the triplet and singlet states. A complete listing of the assigned transitions is available through auxiliary sources. Relative intensities of the individual spin species are obtained from the infrared-infrared double-resonance scans. These values are used since the line density in the single

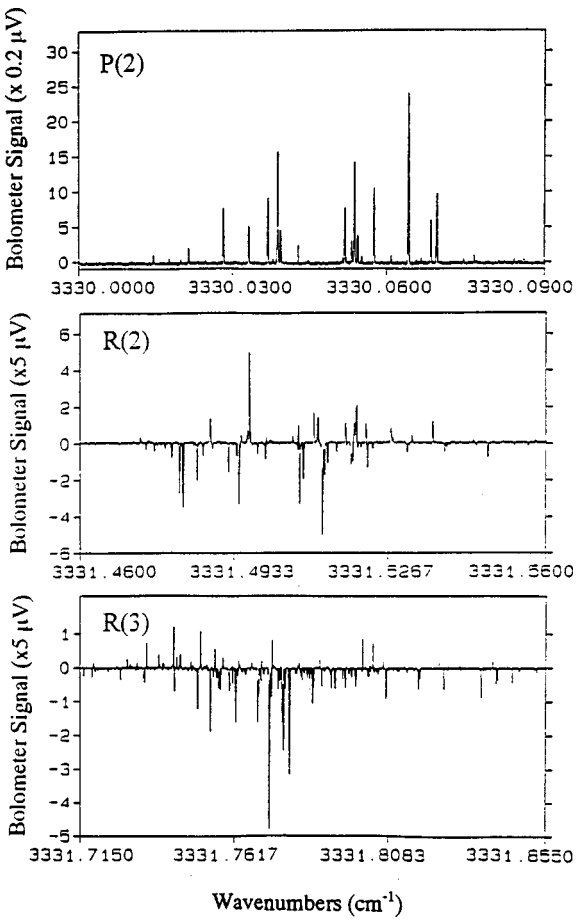


FIG. 6. The other transitions of the acetylenic C–H stretch of propargyl amine near 3330 $cm^{-1}$ that were assigned in this study are shown. The relatively simple $P(1)$ region, which was used to assign the $0_{00}$ states, is not shown. The $R(1)$ region appeared in Fig. 2.

photon spectrum is so high that transitions are frequently overlapped. The relative intensities for $I_H=1$ and $I_H=0$ multiplets for each value of $J$, $K_a$, and $K_c$ are determined from the single-photon spectrum by scaling to a strong, isolated transition of each nuclear-spin modification. This scaling allows comparison to the expected 3:1 intensity ratio.

## V. DISCUSSION

### A. Total intensities of the two nuclear-spin modifications

An assessment of the completeness of the data set is obtained by considering the total intensities for the two nuclear-spin modifications. Nuclear-spin statistics require that the intensity ratio be 3:1. Since the total infrared transition moment is conserved in the IVR fragmentation, the sum of intensities of all components of the IVR multiplet will preserve the 3:1 ratio. The observed ratios, shown in Fig. 7, are observed to be nearly 3:1, indicating that the data set is fairly complete.

Two features of Fig. 7 should be noted. First of all, there is little bias for observing ratios greater than 3:1. It may have been expected that it would be more likely to miss small lines from the singlet nuclear spin modification since weak lines of the IVR multiplet for this modification would fall beneath the noise level faster than weak lines in the triplet modification. The lack of bias to ratios large than 3:1 occurs due to the double-resonance technique. The noise is determined by the monitored 10 $\mu$m transition and is proportional to the signal strength of the monitored transitions.

Second, the largest discrepancies in the 3:1 ratios are truly problematic. The missing intensity is outside limits expected due to the 10% relative intensity precision of the measurements. One cause of poor agreement with the 3:1 statistics could be saturation effects for weakly fragmented transitions, such as the lower $J$ multiplets. Also, it is possible that intensity has been shifted to transitions lying outside the region scanned in double-resonance, as would occur for strong coupling to some more distant vibrational state.

TABLE I. Number of eigenstate transitions assigned to each IVR multiplet, the centers-of-gravity of the multiplets, and the triplet-to-singlet intensity ratio for the multiplets.

| Rovibrational transition | $I_H=0$ $N$ | (singlet) $E_{bright}$ ($cm^{-1}$) | $I_H=1$ $N$ | (triplet) $E_{bright}$ ($cm^{-1}$) | Intensity ratio |
|---|---|---|---|---|---|
| $0_{00}-1_{01}$ | 2 | 3330.33521 | 3 | 3330.33953 | 4.11 |
| $1_{01}-2_{02}$ | 3 | 3330.04808 | 4 | 3330.04894 | 3.79 |
| $1_{11}-2_{12}$ | 5 | 3330.06095 | 3 | 3330.06204 | 2.52 |
| $1_{10}-2_{11}$ | 2 | 3330.03035 | 3 | 3330.0311 | 3.57 |
| $2_{02}-1_{01}$ | 2 | 3331.20525 | 3 | 3331.18765 | 3.01 |
| $2_{12}-1_{11}$ | 6 | 3331.1844 | 5 | 3331.18765 | 3.17 |
| $2_{11}-1_{10}$ | 9 | 3331.21721 | 7 | 3331.22454 | 2.47 |
| $3_{03}-2_{02}$ | 10 | 3331.50822 | 9 | 3331.50932 | 2.90 |
| $3_{13}-2_{12}$ | 9 | 3331.48679 | 12 | 3331.48984 | 3.66 |
| $3_{12}-2_{11}$ | 7 | 3331.52094 | 9 | 3331.52097 | 3.02 |
| $3_{21}-2_{20}$ | 7 | 3331.50888 | 9 | 3331.49994 | 3.22 |
| $4_{04}-3_{03}$ | 9 | 3331.77167 | 7 | 3331.77465 | 3.75 |
| $4_{14}-3_{13}$ | ⋯ | ⋯ | 14 | 3331.74662 | ⋯ |
| $4_{13}-3_{12}$ | 5 | 3331.79905 | 8 | 3331.80658 | 2.26 |
| $4_{22}-3_{21}$ | 11 | 3331.76897 | 14 | 3331.76929 | 3.15 |
| $4_{31}-3_{30}$ | ⋯ | ⋯ | 12 | 3331.76481 | ⋯ |

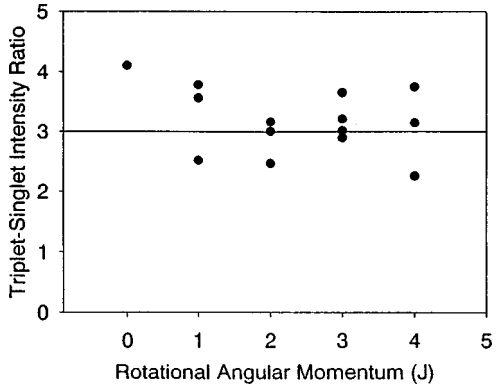


FIG. 7. The measured intensity ratios for the IVR multiplets are shown. This value is the ratio of the sum of the intensities of transitions in the IVR multiplet of the $I_H=1$ species of a single rotational ($J_{Ka,Kc}$) upper state to that of the intensity sum for the $I_H=0$ multiplet. This ratio has the expected value of three based on the nuclear spin statistics of the amino-hydrogen interchange. The ratio determination can be used to estimate the completeness of the spectrum. Ratios far from the expected value of 3 may indicated transition strength borrowed through nonresonant couplings to vibrational states outside the primary $R(J)$ scan region.

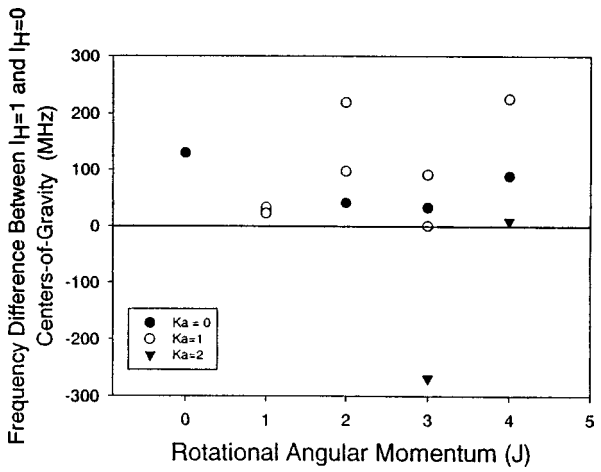


FIG. 8. The frequency difference of the centers-of-gravity of the two spin species for rotational states where both the $I_H=1$ and $I_H=0$ states were assigned are shown. Under the single bright state assumption, this difference reflects the change in tunneling splitting between the ground and excited C–H stretch states. However, in practice, the frequency difference is a signature of nonresonant coupling to bath states with larger tunneling splittings due to excitation in the inversion-internal rotation promoting modes. This effect is seen, for example, in the 10 $\mu$m spectrum of Fig. 5.

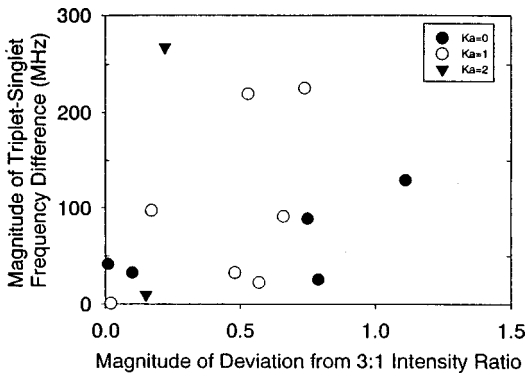


FIG. 9. The magnitude of the center-of-gravity shift for the two spin species is shown vs the deviation of the intensity ratio from 3:1. Large differences between the centers-of-gravity are observed even when the measured intensity ratio is very close to the expected value. In general, the two measures are uncorrelated: the same spread of shifts is observed for small deviations from 3:1 (i.e., 2.8 to 3.2, or deviations from 0.0 to 0.2) as for larger values.

### B. Splittings in the centers-of-gravity for the two nuclear-spin modifications

According to the single bright-state assumption for interpreting IVR spectra, the center-of-gravity of the IVR multiplet resides at the unperturbed position of the bright state transition.[10] In the case of propargyl amine, it is likely that excitation of the acetylenic C–H stretch does not dramatically change the large amplitude potential for motions localized at the other end of the molecule. As a result, the centers-of-gravity for the two nuclear spin modifications are expected to be the same. This assumption has been used to interpret and assign other fragmented spectra of molecules with high barrier, large amplitude motions.[7,21]

However, in practice, these centers-of-gravity may not coincide when experimental data is used. Instead, an ''effective'' splitting can be observed due to nonresonant vibrational coupling to vibrational bath states with high levels of excitation in the large amplitude vibrations which have large tunneling splittings.[22] Even in unfragmented spectra at lower levels of excitation, it is often impossible to experimentally detect the perturbing state due to the low intensity borrowed from the bright state. Frequency-shifting is the more easily observed characteristic of this coupling.[14]

The frequency differences of the centers-of-gravity of the transitions of propargyl amine are shown in Fig. 8. These differences measure the change in tunneling splitting in the upper state relative to the ground vibrational state. In all but one measurement, the triplet state lies to higher frequency. The average value of the splitting is about 50 MHz. The same sign of the difference is observed regardless of whether the intensity ratios are greater or less than 3:1. Additionally, large singlet–triplet splittings are observed in cases where the intensity ratio is very close to 3:1. Figure 9 shows a scatter plot illustrating the lack of correlation between the size of the tunneling splitting difference and the deviation from the expected 3:1 intensity ratio for the two tunneling state symmetries.

The differences in the centers-of-gravity for the singlet and triplet states are caused by missing transitions outside the scanned spectral range. Using the data for the $3_{03}-2_{02}$ ($I_H=1$) IVR multiplet, we have estimated the effect of experimental intensity uncertainty of the measured transitions on the center-of-gravity position. Ten calculations of the center-of-gravity were made after placing random 0% to $\pm 10\%$ errors on the intensities. The standard deviation of the calculated center-of-gravity is only 3 MHz and, therefore, cannot account for our experimental observations of splittings of 10 MHz to 200 MHz. We conclude that nonresonant coupling to a vibration, or a set of vibrations, with large amounts of excitation in motions localized at the amine end of the are important in the IVR dynamics of the acetylenic C–H stretch of propargyl amine. These vibrational states will have a large tunneling splitting which can differentially shift the effective centers-of-gravity for the two nuclear-spin modifications. The current poor knowledge of the large amplitude surface prevents further speculation on the identity of this state (or states). In this way, the same effects causing nuclear-spin splittings in the 10 $\mu$m spectra of primary amines,[14] survive into energy regions showing extensive IVR.

### C. Density of coupled states

The density of states is a key quantity in statistical theories of unimolecular reaction. The ability to calculate this quantity for large molecules can be tested by eigenstate-resolved spectroscopy since the state density is directly available from the spectrum. However, eigenstate-resolved spectra generally display a $J$-dependent state density that reflects the presence of rovibrational interactions (Coriolis or centrifugal coupling, for example). To compare the measured and calculated state density, we extrapolate the measured state density to $J=0$ where only anharmonic interactions can

occur. In propargyl amine, the value of the state density at $J=0$ gives the density of states with $A'$ symmetry and is half the total state density of the molecule.

The form of the $J$-dependence of the state density contains information about the type of rovibrational mechanism involved in the IVR process. For example, if only anharmonic interactions were present, the state density would not vary with the total angular momentum, $J$. When Coriolis interactions about all three principal axes are operative, then the state density is expected to grow as

$$\rho(J)=\rho_0(2J+1), \tag{1}$$

where $\rho_0$ is the density at $J=0$.

Other types of a $J$-dependence between these limiting cases are also possible. In particular, there can still be a growth in the state density as a function of the total angular momentum even if only anharmonic interactions occur. In this case, coupling between states with different values of the $K_a$-quantum number can occur due to ''nonorthogonality'' of the rotational wave functions. This nonorthogonality can be caused by the rotation of the inertial axes corresponding to internal rotation,[23,24] as discussed by Li, Ezra, and Philips.[25] These affects can also be caused by changes in the asymmetry term in the rotational Hamiltonian, $(B-C)$, for each normal-mode vibrational states.[26] If all rotational levels of the same parity and same vibrational symmetry (because only anharmonic interaction occur) appear in the spectrum, then the $J$-dependence of the state density for the $K_a=0$ spectra is

$$\rho(J)=\rho_0(J+1), \tag{2}$$

where, again, $\rho_0$ is the state density at $J=0$.

We have determined the experimental state densities for each $|JK_aK_c;I_H\rangle$ level through the expression

$$\rho=\frac{N-1}{\Delta E}, \tag{3}$$

where $N$ is the number of eigenstates in the IVR multiplet and $\Delta E$ is the energy difference between the first and last eigenstate in the spectrum. This quantity is equivalent to calculating the average next-nearest-neighbor level spacing in the spectrum. The finite signal to noise ratio of the measurement makes it possible that states are missed in the spectrum, making this value a lower limit. In the present study we have measured the infrared spectrum at two different sensitivities as shown in Figs. 1 and 2. We note that for the $2_{11}$ level, we have assigned no transitions that were not already observed in the lower signal to noise spectrum (the spectrum without using state-focusing has a sensitivity that is lower by a factor of 11). This result suggests that for our highest sensitivity measurements we have observed all of the states in the measured region. The experimental state densities are listed in Table II.

From the present data set, which extends only to $J=4$ we cannot distinguish between the $J$-dependence represented by Eqs. (1) and (2). In our determination of the $J$-dependence we have used only the higher sensitivity $K_a=0$ and $K_a=1$ data. If the full $(2J+1)$-growth form is used, the $J=0$ state density is 22(2) states/cm$^{-1}$ (the value in parenthesis is the type A standard uncertainty with coverage factor, $k=1$). For a $J$-dependence of the form of Eq. (2), the $J=0$ state density is 38(3) states/cm$^{-1}$. In the next section we show that the IVR rates are $K_a$-dependent suggesting the presence of parallel Coriolis ($a$-axis) interaction between the bright and bath states. Because this type of interaction is present, the state density is expected to follow Eq. (1) and we determine the $J=0$ state density to be 22 states/cm$^{-1}$. In the structurally similar molecule propargyl alcohol, we have measured the state densities to $J=9$ and find that the density increases according to Eq. (1).[27] The experimental state densities and this best fit result are shown in Fig. 10.

TABLE II. The experimental density of states for different rotational states of the acetylenic C–H stretch.

| Rotational level ($J_{Ka,Kc}$) | State density $I_H=0$ (states/cm$^{-1}$) | State density $I_H=1$ (states/cm$^{-1}$) | Average state density (states/cm$^{-1}$) |
|---|---|---|---|
| $0_{00}$ | 45 | 55 | 50 |
| $1_{01}$ | 94 | 93 | 93 |
| $1_{11}$ | 104 | 222 | 163 |
| $1_{10}$ | 58 | 86 | 72 |
| $2_{02}$ | 122 | 71 | 97 |
| $2_{12}$ | 164 | 126 | 145 |
| $2_{11}$ | 134 | 75 | 105 |
| $3_{03}$ | 148 | 222 | 185 |
| $3_{13}$ | 230 | 162 | 196 |
| $3_{12}$ | 93 | 112 | 103 |
| $3_{21}$ | 73 | 111 | 92 |
| $4_{04}$ | 182 | 256 | 219 |
| $4_{14}$ | ⋯ | 200 | ⋯ |
| $4_{13}$ | 91 | 109 | 100 |
| $4_{22}$ | 98 | 175 | 137 |
| $4_{31}$ | ⋯ | 185 | ⋯ |

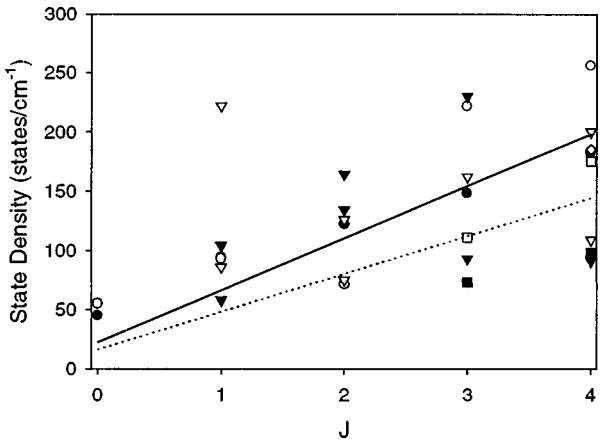


FIG. 10. The measured state densities for the IVR multiplets of propargyl amine are shown. The open symbols are the values for the triplet spin state ($I_H=1$). The $K_a$ values are denoted by the symbol shape; $K_a=0$, circle; $K_a=1$, triangle; $K_a=2$, square; and $K_a=3$, diamond. The dotted line gives the $(2J+1)$ growth of the state density when the calculated density of $A'$ states is used (16 states/cm$^{-1}$). The solid line gives the best fit for a $(2J+1)$ growth in the state density with the density of $A'$ states of 22 states/cm$^{-1}$. The best-fit determination uses only the high sensitivity $K_a=0$ and $K_a=1$ data.

### D. Comparison of the measured and calculated state densities

Near 3300 $cm^{-1}$ the experimental determination of the density of $A'$ vibrational states is 22 states/$cm^{-1}$. This value can be compared to the calculated state density of $A'$ vibrational states, 16 states/$cm^{-1}$. The expected $J$-dependent state density using this calculated value is also shown in Fig. 10. The calculation assumes a harmonic approximation for the normal modes excluding the torsion, which is treated separately. The normal mode frequencies used in the calculation are from the previous assignment of the infrared spectrum of propargyl amine.[20] The torsional energy levels are determined from diagonalization of the torsional Hamiltonian in a free rotor basis set ($M_{max}=50$) using an $F$ value of 9.2777 $cm^{-1}$ and *ab initio* values for the first three Fourier coefficients of the potential, $V_1=-824.8\ cm^{-1}$, $V_2=430.0\ cm^{-1}$, and $V_3=-643.3\ cm^{-1}$.[28] This *ab initio* potential predicts the fundamental torsional band of the *trans* form at 260 $cm^{-1}$. The torsion has been assigned in the infrared spectrum to a band at 334 $cm^{-1}$ based on its *c*-type band contour. This comparison suggests the *ab initio* torsional potential overestimates the calculated state density. The density of states is determined by a direct state count, treating the torsional coordinate separately. Despite the likely overestimate from the low calculated torsional frequency, the measured state density is still 37% larger than the calculated value. The neglect of diagonal and off-diagonal anharmonicity is a major source of error in the calculated values of state densities and is the likely source of this difference.

### E. Measurement of the IVR lifetime

Perhaps the most important quantity determined from the frequency-resolved spectrum is the homogeneous IVR lifetime, which measures the time scale of energy localization in the bright state following short-pulsed excitation of the acetylenic C–H stretching vibration. When the eigenstates of the spectrum can be assigned to a single, rovibrational-torsional state of the vibrationally excited bright-state it is possible to calculate the time evolution of this state from information contained in the frequency-resolved spectrum.[7,8,10,21]

When the IVR multiplet contains more than about 5 eigenstates, the time evolution displays the characteristics of intermediate case IVR.[29] There are two general features expected for these survival probability decays.[30] At early times there is a near exponential decay of the probability of having the energy localized in the bright state. The IVR lifetime is given as the $1/e$ point of this initial decay. The IVR lifetime is reflected in the overall width of the IVR multiplet. At longer times, the time evolution will show structure from the beating between the individual eigenstates. In the egalitarian model, it can be shown that this structure oscillates around the value $(1/N)$, where $N$ is the number of eigenstates in the IVR multiplet. This value is just the straight probability of finding the molecule in one of $N$ coupled states. As the number of eigenstates increases, this beat structure becomes much smoother and the evolution approaches a single exponential decay. At the same time the line shape of the IVR multiplet becomes smoother and becomes Lorentzian with a width determined by the IVR rate.[12]

Two methods for determining the IVR lifetime are from the calculation of the survival probability[11] or from the Fermi Golden Rule expression of the IVR rate,

$$\Gamma = 2\pi\langle W^2\rangle\rho. \tag{4}$$

To calculate the IVR rate from this expression the mean-squared matrix element and the state density must be determined. Both of these quantities can be determined from a fully assigned spectrum. (This assignment must include the nuclear spin labels for the different large amplitude tunneling states.) The determination of the state density was presented above. The mean-squared matrix element is calculated using the algebraic formulation[31] of the Lawrance–Knight deconvolution method.[32]

The experimental lifetimes determined by these two methods for IVR multiplets containing 5 or more eigenstates

TABLE III. IVR lifetimes for the acetylenic C–H stretch of propargyl amine for multiplets containing at least five eigenstates.

| | $I_H=0$ | | | $I_H=1$ | | |
|---|---|---|---|---|---|---|
| Rotational level ($J_{KaKc}$) | Survival probability lifetime (ps) | Golden Rule lifetime (ps) | Scaled survival probability (ps) | Survival probability lifetime (ps) | Golden Rule lifetime (ps) | Scaled survival probability (ps) |
| $1_{11}$ | 570 | 394 | 341 | ⋯ | ⋯ | ⋯ |
| $2_{12}$ | 615 | 344 | 368 | 585 | 333 | 350 |
| $2_{11}$ | 430 | 267 | 257 | 260 | 145 | 156 |
| $3_{03}$ | 725 | 467 | 434 | 735 | 499 | 440 |
| $3_{13}$ | 825 | 413 | 494 | 455 | 330 | 272 |
| $3_{12}$ | 715 | 268 | 428 | 330 | 233 | 198 |
| $3_{21}$ | 530 | 140 | 317 | 400 | 267 | 239 |
| $4_{04}$ | 550 | 381 | 329 | 970 | 617 | 580 |
| $4_{14}$ | ⋯ | ⋯ | ⋯ | 450 | 338 | 269 |
| $4_{13}$ | 945 | 450 | 566 | 495 | 328 | 296 |
| $4_{22}$ | 255 | 167 | 152 | 250 | 137 | 150 |
| $4_{31}$ | ⋯ | ⋯ | ⋯ | 545 | 312 | 326 |

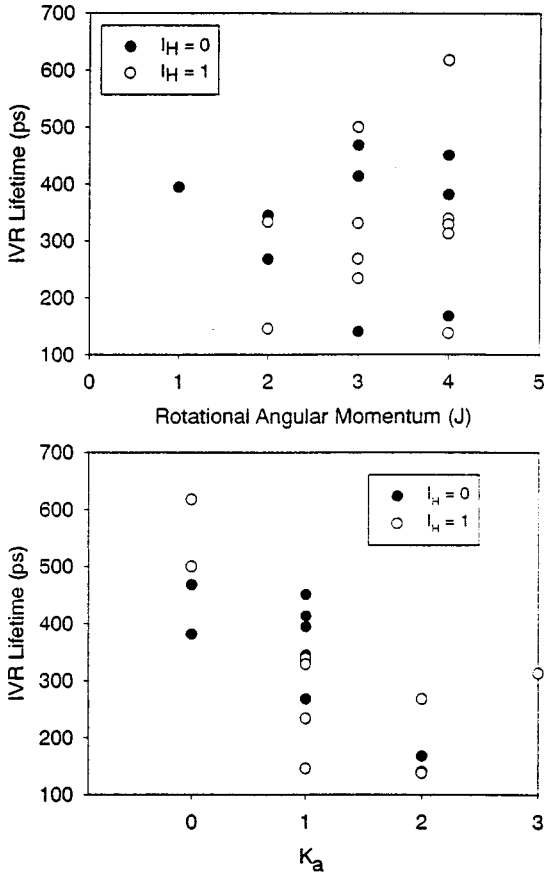


FIG. 11. The calculated IVR lifetimes for IVR multiplets containing at least 5 molecular eigenstates are plotted as a function of $J$ (upper panel) and $K_a$ (lower panel). The lifetime values used are those calculated from the Golden Rule formula (see Table VI and the discussion in the text for the relationship of these values from those determined from the survival probability). There appears to be a $K_a$-dependent lifetime with the IVR-rate increasing as $K_a$ increases. There is no apparent $J$-dependence. (Much of the scatter in the top plot is due to the multiple values of $K_a$ that occur for each value of $J$.)

appear in Table III. When the IVR multiplet contains a small number of eigenstates, the lifetime calculated using the Golden Rule approach is consistently faster than the survival probability method. In Table III, an empirical scale factor of 0.6, chosen to achieve best agreement between the two calculated values, is applied to the survival probability measurements to show that the two methods give the same data trends. Numerical simulations show that as more states are included further in the wings of a Lorentzian line shape profile, the two calculations converge to the value given by Eq. (4). The large discrepancies between the values for $3_{12}$ and $3_{21}$ (both $I_H=0$) can be traced to recurrence structure in the survival probability that prevents the initial decay from falling smoothly below the $1/e$ point.

From this data set we can assess whether the lifetime depends on the nuclear spin species. This type of dependence could potentially arise from two factors: (1) Since the wave functions of the different nuclear spin species sample different spatial regions of the large amplitude potential, the coupling matrix elements could have a nuclear spin symmetry dependence. (2) If there were a strong coupling to a state with large amounts of excitation in the large amplitude coordinate (causing a larger tunneling splitting in the coupled state), then the amount of this state mixed into the different spin species of the acetylenic C–H stretch would be different. This state's contribution to the total IVR rate of the acetylenic C–H stretch would then be different for the two different spin modifications. The average lifetimes for the Golden Rule calculated data in Table III are 329(114) ps for $I_H=0$, 322(140) ps for $I_H=1$, and 325(125) ps for the full data set. There is no evidence of a nuclear spin-dependent IVR rate. For the following discussion of the rotational dependence of the IVR rate, data from both spin symmetries are combined.

One advantage of frequency-resolved methods is that the lifetimes are determined with full state-specificity, allowing the rotational-dependence (or nuclear-spin modification-dependence) of the IVR rates to be uncovered. The lifetimes are shown in Fig. 11 as a function of $J$ and $K_a$. There appears to be no trend in the lifetime for the $J$ quantum label. However, there is an apparent increase in the IVR rate as $K_a$ increases. The *lifetime* averages for different $K_a$ states are 491(98) ps for $K_a=0$, 320(83) ps for $K_a=1$, and 178(61) ps for $K_a=2$. The experimental $K_a$-dependent (for $K_a=0-2$) IVR *rate* is approximately

$$\Gamma(K_a)=\Gamma_{\text{anh}}+(0.5)\Gamma_{\text{anh}}K_a^2. \tag{5}$$

The lack of data for higher $K_a$ values prevents us from being able to fit to this form. In particular, the dependence of the rate on $K_a^2$ is not well established, however, it represents the data better than a linear $K_a$-dependence.

### F. Statistical measures of the spectrum

In cases where the spectrum is extensively perturbed, it is no longer practical to attempt a rigorous spectroscopic analysis to assign the vibrational and $K$ rotational quantum numbers of the perturbing states and determine the coupling matrix elements between the states. Instead, it is hoped that general features about the vibrational dynamics can be learned from the statistical properties of the spectrum using methods originally developed to interpret nuclear spectra.[33] These statistical methods involve analyzing the fluctuations in the eigenvalue spacings and the intensities (or dissociation widths) of the transitions. Connections between the statistical properties of the spectrum and the chaotic nature of the underlying classical dynamics have been made in several recent studies of highly excited atoms in external fields.[34,35]

Level spacing statistics usually focus on the distribution of the nearest neighbor spacings in a homogeneous series of eigenvalues. A Poisson spacing distribution suggest regular dynamics in the energy range, whereas a Wigner distribution, which results from a linear repulsion of eigenstates, suggests chaotic dynamics.[36] For these methods to be applicable, it is necessary that all good (or approximately good) quantum numbers are the same for members of the series. In terms of molecular spectra, the states must have the same rotational and nuclear-spin quantum numbers (if torsional tunneling is possible). Our assigned spectra meet these criteria. In Table IV, the moments of the nearest neighbor spacings for the IVR multiplets containing five or more eigenstates are presented. The moments of the distribution are

TABLE IV. Moments of the level spacing distribution for IVR multiplets with five or more eigenstates.

| Rotational level | $I_H=0$ | | | $I_H=1$ | | |
|---|---|---|---|---|---|---|
| | $\langle s^2\rangle/\langle s\rangle^2$ | $\langle s^3\rangle/\langle s\rangle^3$ | $\langle s^4\rangle/\langle s\rangle^4$ | $\langle s^2\rangle/\langle s\rangle^2$ | $\langle s^3\rangle/\langle s\rangle^3$ | $\langle s^4\rangle/\langle s\rangle^4$ |
| $1_{11}$ | 1.34 | 1.91 | 2.81 | ⋯ | ⋯ | ⋯ |
| $2_{12}$ | 1.02 | 1.07 | 1.15 | 1.08 | 1.24 | 1.53 |
| $2_{11}$ | 1.28 | 1.82 | 2.78 | 1.49 | 2.71 | 5.52 |
| $3_{03}$ | 1.99 | 5.61 | 18.2 | 1.28 | 1.83 | 2.79 |
| $3_{13}$ | 1.63 | 3.51 | 8.68 | 2.12 | 6.47 | 30 |
| $3_{12}$ | 2.33 | 7.47 | 25.9 | 1.38 | 2.16 | 3.6 |
| $3_{21}$ | 1.82 | 4.44 | 12.1 | 1.16 | 1.46 | 1.93 |
| $4_{04}$ | 1.32 | 2.13 | 3.84 | 1.23 | 1.69 | 2.49 |
| $4_{14}$ | ⋯ | ⋯ | ⋯ | 1.2 | 1.62 | 2.33 |
| $4_{13}$ | 2.28 | 6.15 | 17.4 | 1.97 | 5.42 | 16.7 |
| $4_{22}$ | 1.74 | 4.25 | 12.2 | 1.34 | 2.29 | 4.54 |
| $4_{31}$ | ⋯ | ⋯ | ⋯ | 1.91 | 5.73 | 20.3 |
| Wigner | 1.26 | 1.91 | 3.25 | | | |
| Poisson | 2 | 6 | 12 | | | |

used since they provide a scale between the two limits.[37] This scale can be related to the number of missing or spurious levels in the sequence. In the present data set where definitive assignments are made through double-resonance techniques, the scale should indicate missing levels.

The results in Table IV show that the use of level spacing statistics in this spectrum are of little use in characterizing the dynamics of the system. The experimental moments of the distribution cover the entire range from Poisson to Wigner, and beyond. Similar large variations in the level spacing statistics have been observed in the $3\nu_1$ spectrum of propyne[38] and were ascribed to a multilevel hierarchy in the coupling matrix elements.[39–41] In our case, a hierarchy that separates anharmonic couplings with $\Delta K_a=0$ from the anharmonic couplings with $\Delta K_a\neq 0$ that are driven by rotational nonorthogonality could possibly explain these statistics.

The intensities of the individual eigenstates should also show fluctuations in the case of chaotic dynamics. The transition intensities should be $\chi^2$-distributed about the smooth Lorentzian profile determined by the IVR rate.[33] Heller has presented a statistic, *F*, that is related to the intensity distribution.[42] This statistic has the interpretation of measuring the fraction of phase space covered by the dynamics. Due to quantum interference effects, which lead to the intensity distribution, a chaotic system should sample only 1/3 of the available phase space. As discussed by Heller,[42] the fraction of phase space sampled can be estimated by comparing the effective number of transitions observed in the spectrum,

$$N_{\text{eff}}=\Sigma I_i^2/(\Sigma I_i)^2 \tag{6}$$

to the total number of accessible states. This latter quantity can be estimated as the product of the IVR rate determined from Fermi's Golden Rule,

$$\Gamma=(2\pi/h)\langle W^2\rangle\rho \tag{7}$$

and the time required for the quantum dynamics to finish their nontrivial evolution. This ''break time''

$$\tau_B=2\pi h\rho \tag{8}$$

is the time required for the system to resolve the individual eigenstates.

For the analysis we only require the root-mean-squared coupling matrix element for the multiplet. This quantity is determined using the Lawrance–Knight deconvolution method.[31,32] This method is applicable only when the spectra arise from a single bright state. In particular, the nuclear spin labels due to torsion-inversion tunneling must be separately assigned. The results for the *F* statistic are given in Table V for all multiplets containing at least 5 eigenstates. The average over all 20 determinations is 0.312(88), in good agreement with the value of 1/3 expected for a chaotic system.

The agreement of the intensity-related *F* statistic to the expectations of a chaotic system is in contrast to the results for the level spacing statistics. In a careful study of the properties of random matrix Hamiltonians for molecular spectroscopy, Perry has noted that the intensity statistics are the first to converge to the random matrix limit as the root-mean-squared interaction matrix element is increased.[43] Our results are consistent with this previous work. We also find that there is a slower contribution to the IVR rate from parallel Coriolis interactions. The presence of two types of coupling matrix elements, one for anharmonic and one for Coriolis

TABLE V. Calculated values of the *F*-statistic for IVR multiplets containing five or more eigenstates.

| Rotational level | $F(I_H=0)$ | $F(I_H=1)$ |
|---|---|---|
| $1_{11}$ | 0.39 | ⋯ |
| $2_{12}$ | 0.24 | ⋯ |
| $2_{11}$ | 0.37 | 0.23 |
| $3_{03}$ | 0.37 | 0.27 |
| $3_{13}$ | 0.21 | 0.42 |
| $3_{12}$ | 0.28 | 0.34 |
| $3_{21}$ | 0.34 | 0.38 |
| $4_{04}$ | 0.26 | 0.35 |
| $4_{14}$ | ⋯ | 0.24 |
| $4_{13}$ | 0.48 | 0.47 |
| $4_{22}$ | 0.31 | 0.22 |
| $4_{31}$ | ⋯ | 0.47 |

interactions, is also expected to skew the level spacing statistics.[44] Dual matrix element distributions can lead to a hierarchical structure in the spectrum and the development of theoretical analysis tools for this case may be more applicable to this spectrum.[39–41]

## VI. CONCLUSIONS

We have presented the analysis of the fully assigned acetylenic C–H spectrum of propargyl amine. Using infrared–infrared double-resonance spectroscopy we have been able to assign both the rotational and nuclear spin quantum numbers to each molecular eigenstate in the infrared spectrum. We observe a $J$-dependent growth in the measured state density, with a $J=0$ density determined to be 22 states/cm$^{-1}$. This value is about 40% higher than a direct count calculation. The $K_a=0$ IVR lifetime is about 500 ps and the lifetime decreases with the $K_a$-quantum number. This rotational dependence indicates that the acetylenic C–H stretch bright-state can couple to near-resonant bath states through an $a$-axis Coriolis mechanism.

The measured IVR lifetime for the acetylenic C–H stretch in propargyl amine is similar to the lifetime of other acetylenic compounds.[10] For example, in the series of compounds $HCCCH_2X$ ($X=CH_3$,[6,7] OH,[27] and $NH_2$) the IVR lifetimes are 200 ps, 400 ps, and 500 ps, respectively. The lifetime of $(CH_3)_3CCCH$ (200 ps) (Ref. 12) and the lifetimes in the two isomeric forms of 1-pentyne (*trans* 440 ps and *gauche* 240 ps) (Ref. 7) are also on the same order. Although these results suggest the idea of a chromophore-dependent IVR rate, two ''counterexamples'' are known; $(CD_3)_3CCCH$ (40 ps) (Ref. 45) and $(CF_3)_3CCCH$ (60 ps).[46] The cause for the similarity in the lifetimes of several of these molecules has yet to be determined,[47,48] but recent theoretical efforts suggest that it would be possible to determine whether are special set of low-order resonances related to the vibrations of the acetylenic chromophore that make similar and dominant contributions to the IVR rates in this structural series.[5,49]

The determined IVR rates for the two different torsional species are roughly the same (for the same values of $K_a$). This result indicates that the IVR rate is determined by coupling to more distant, nonresonant vibrational states. Since different bath states have different torsion-inversion splittings, the exact vibrational make-up of the near-resonant states will be different for the two spin modifications. The fact that the frequency degeneracy for the transitions to the two nuclear spin species is lifted (i.e., each eigenstate can be uniquely assigned as a singlet or triplet state) illustrates this result.[50] Therefore, the direct, near-resonant couplings are not the controlling factor in the IVR rate, although they may cause fluctuations about the average IVR rate. On a more distant, coarse grained scale, the differences in tunneling splittings of the two spin species of a vibration become relatively less important and the two components contribute roughly equally to the dynamics of the acetylenic C–H stretch.

There is evidence that states involving excitation in the large amplitude coordinates are playing a role in the IVR process. The spectroscopic signature of coupling to these states is a residual ''effective'' singlet–triplet nuclear spin splitting difference in the centers-of-gravity of the IVR multiplets.[22] The average value of the difference is about 100 MHz, with the triplet state higher in frequency in all but one case. Vibrations that promote inversion-internal rotation exhibit large singlet–triplet splitting difference, as found in the 10 $\mu$m spectrum.[14] Nonresonant coupling to these states produces the observed ''effective'' splitting in the 3.0 $\mu$m spectrum. However, despite this differential coupling, there is no nuclear-spin dependence to the IVR rate.

A statistical analysis of the spectrum has produced ambiguous results over whether the dynamics are chaotic. The intensity-related statistic, $F$,[42] shows very good agreement with the expectations of a chaotic spectrum. However, the level spacing statistics provide no indication of whether the dynamics are regular or chaotic. The cause of these different conclusions could be the existence of well-defined levels of coupling to the vibrational bath. Future developments of hierarchical analysis methods will be required to extract this information from the spectrum.[41]

## ACKNOWLEDGMENT

One of us (B.H.P.) acknowledges a NRC Postdoctoral Fellowship for support during this work.

[1] P. J. Robinson and K. A. Holbrook, *Unimolecular Reactions* (Wiley–Interscience, New York, 1972), Chap. 4.
[2] A. Sinha, M. C. Hsiao, and F. F. Crim, J. Chem. Phys. **92**, 6333 (1990).
[3] M. J. Bronikowski, W. R. Simpson, and R. N. Zare, J. Phys. Chem. **97**, 2194 (1992).
[4] A. Sinha, J. D. Thoemke, and F. F. Crim, J. Chem. Phys. **96**, 372 (1993).
[5] A. A. Stuchebrukhov and R. A. Marcus, J. Chem. Phys. **98**, 6044 (1993).
[6] A. M. de Souza, D. Kaur, and D. S. Perry, J. Chem. Phys. **88**, 4569 (1988).
[7] A. McIlroy and D. J. Nesbitt, J. Chem. Phys. **92**, 2229 (1990).
[8] B. H. Pate, K. K. Lehmann, and G. Scoles, J. Chem. Phys. **95**, 3891 (1991).
[9] C. L. Brummel, S. W. Mork, and L. A. Philips, J. Chem. Phys. **95**, 7041 (1991).
[10] K. K. Lehmann, G. Scoles, and B. H. Pate, Annu. Rev. Phys. Chem. **45**, 241 (1994).
[11] H. L. Kim, T. J. Kulp, and J. D. McDonald, J. Chem. Phys. **87**, 4376 (1987).
[12] E. R. Th. Kerstel, K. K. Lehmann, T. F. Mentel, B. H. Pate, and G. Scoles, J. Phys. Chem. **95**, 282 (1991).
[13] R. Cervellati, W. Caminati, C. D. Esposti, and A. M. Mirri, J. Mol. Spectrosc. **66**, 389 (1977).
[14] A. M. Andrews, G. T. Fraser, and B. H. Pate, J. Phys. Chem. **98**, 9979 (1994).
[15] G. T. Fraser and A. S. Pine, J. Chem. Phys. **91**, 637 (1989).
[16] G. T. Fraser and B. H. Pate, J. Chem. Phys. **98**, 2477 (1993).
[17] J. Reuss, *State Selection by Nonoptical Means*, Vol. 1 in *Atomic and Molecular Beam Methods*, edited by G. Scoles (Oxford University Press, New York, 1988).
[18] G. T. Fraser, A. S. Pine, and W. A. Kreiner, J. Chem. Phys. **94**, 7061 (1991).
[19] For a list of references on the inversion-internal rotation motions of methyl amine, see M. Kreglewski and G. Wlodarczak, J. Mol. Spectrosc. **156**, 383 (1992).
[20] Y. Hamada, M. Tsuboi, M. Nakata, and M. Tasumi, J. Mol. Spectrosc. **107**, 269 (1984).
[21] G. A. Bethardy and D. S. Perry, J. Chem. Phys. **98**, 6651 (1993).
[22] A. Ainetschian, G. T. Fraser, J. Ortigoso, and B. H. Pate, J. Chem. Phys. **100**, 729 (1994).
[23] P. Meakin, D. O. Harris, and E. Hirota, J. Chem. Phys. **51**, 3775 (1969).
[24] C. R. Quade and C. C. Lin, J. Chem. Phys. **38**, 540 (1963).
[25] H. Li, G. S. Ezra, and L. A. Philips, J. Chem. Phys. **97**, 5956 (1992).

[26] C. C. Miller, L. A. Philips, A. M. Andrews, G. T. Fraser, B. H. Pate, and R. D. Suenram, J. Chem. Phys. **100**, 831 (1994).
[27] E. Hudspeth, D. A. McWhorter, and B. H. Pate, J. Chem. Phys. **109**, 4316 (1998), this issue.
[28] N. V. Riggs, Aust. J. Chem. **40**, 435 (1987).
[29] F. Lahmani, A. Tramer, and C. Tric, J. Chem. Phys. **60**, 4431 (1974).
[30] K. F. Freed and A. Nitzan, J. Chem. Phys. **73**, 4765 (1980).
[31] K. K. Lehmann, J. Phys. Chem. **95**, 7556 (1991).
[32] W. D. Lawrance and A. E. W. Knight, J. Phys. Chem. **89**, 917 (1985).
[33] C. E. Porter, *Statistical Theories of Spectra: Fluctuations* (Academic, New York, 1965).
[34] H. Friedrich and D. Wintgen, Phys. Rep. **183**, 37 (1989).
[35] A. Holle, J. Main, G. Wiebusch, H. Rottke, and K. H. Welge, Phys. Rev. **61**, 161 (1988).
[36] M. V. Berry, Proc. R. Soc. London, Ser. A **400**, 229 (1985).
[37] K. K. Lehmann and S. L. Coy, J. Chem. Phys. **87**, 5415 (1987).
[38] J. Gambogi, E. R. Th. Kerstel, K. K. Lehmann, and G. Scoles, J. Chem. Phys. **100**, 2612 (1994).
[39] M. J. Davis, G. A. Bethardy, and K. K. Lehmann, J. Chem. Phys. **101**, 2642 (1994).
[40] K. Yamanouchi, N. Ikeda, S. Tsuchiya, D. M. Jonas, J. K. Lundberg, G. W. Adamson, and R. W. Field, J. Chem. Phys. **95**, 6330 (1991).
[41] M. J. Davis, J. Chem. Phys. **98**, 2614 (1993).
[42] E. J. Heller, J. Chem. Phys. **92**, 1718 (1990).
[43] G. A. Bethardy and D. S. Perry, J. Chem. Phys. **99**, 9400 (1993).
[44] B. H. Pate, Ph.D. thesis, Princeton University, 1992.
[45] J. E. Gambogi, R. P. L'Esperance, K. K. Lehmann, B. H. Pate, and G. Scoles, J. Chem. Phys. **98**, 1116 (1993).
[46] J. E. Gambogi, K. K. Lehmann, B. H. Pate, G. Scoles, and X. Yang, J. Chem. Phys. **98**, 1748 (1993).
[47] G. A. Bethardy, X. Wang, and D. S. Perry, Can. J. Chem. **72**, 652 (1994).
[48] D. S. Perry, G. A. Bethardy, and X. Wang, Ber. Bunsenges. Phys. Chem. **99**, 530 (1995).
[49] A. A. Stuchebrukhov, A. Mehta, and R. A. Marcus, J. Phys. Chem. **97**, 12491 (1993).
[50] See AIP Document No. E-PAPS-JCPSA6-109-010835 for a complete listing of the transition frequencies and intensities of this spectrum. E-PAPS document files may be retrieved free of charge from our FTP server (http://www.aip.org/epaps/epaps.html) or from ftp.aip.org in the directory /epaps/. For further information: e-mail: paps@aip.org or fax: 516-576-2223.